Electronic Supplementary Information

Experimental section

Materials.

$NiCl_2 \cdot 6H_2O$, VCl_3, NaOH, Formamide and Ethyl alcohol were purchased from Sinopharm Chemical Reagent Co. Ltd. Urea, RuO_2, Pt/C and 5 wt% Nafion solution were purchased from Sigma-Aldrich. NF was purchased from Guangjiayuan Co. Ltd. GO was purchased from Jicang Nano Co. Ltd. The water used in all experiments was deionized water. All the chemicals were used as received without further purification.

Synthesis of V-α-$Ni(OH)_2$/GO.

A 10 mL aqueous solution containing 1.738 g $NiCl_2 \cdot 6H_2O$ and 0.393 g VCl_3 was added dropwise to 20 mL aqueous solution containing 90 mg GO and 5 ml formamide under magnetic stirring at 85 °C. At the same time, 2.5 M NaOH was added dropwise into the solution to maintain a pH of 9.5~10.5. The reaction was completed in 10 min. After cooling to room temperature, the products were washed with ethanol and water several times, collected by centrifugation, and freeze-dried to obtain the V-α-$Ni(OH)_2$/GO.

Synthesis of β-$Ni(OH)_2$/GO.

A 10 mL aqueous solution containing 2.377 g $NiCl_2 \cdot 6H_2O$ and was added dropwise to 20 mL aqueous solution containing 90 mg GO and 5 ml formamide under magnetic stirring at 85 °C. At the same time, 2.5 M NaOH was added dropwise into the solution to maintain a pH of 9.5~10.5. The reaction was completed in 10 min. After cooling to room temperature, the products were washed with ethanol and water several times, collected by centrifugation, and freeze-dried to obtain the β-$Ni(OH)_2$/GO.

Synthesis of α-$Ni(OH)_2$/GO.

A 10 mL aqueous solution containing 2.377 g $NiCl_2 \cdot 6H_2O$ and 3 g urea was added dropwise to 20 mL aqueous solution containing 90 mg GO and 5 ml formamide under magnetic stirring at 85 °C and refluxed for 5 hours. After cooling to room temperature, the products were washed with ethanol and water several times, collected by centrifugation, and freeze-dried to obtain the α-$Ni(OH)_2$/GO.

Structure Characterization.

X-ray diffraction (XRD) was performed on Smart Lab 3KW diffractometer with Cu-Kα radiation. Scanning electron microscopy (SEM) was observed on thermo scientific Apreo 2C. Energy dispersive spectroscopy (EDS) was observed on SUPER X. Transmission electron microscopy (TEM) and high-resolution TEM (HRTEM) images were acquired with Talos F200S. X-ray photoelectron spectroscopy (XPS) was investigated by using Thermo Fisher ESCALAB Xi+. Inductively coupled plasma atomic emission spectrometry (ICP) was performed with inductively coupled plasma OES spectrometer (ICP-OES, PE Avio 200) to analyze the elemental composition of the materials. Infrared Spectroscopy (IR) was performed by Nicolet iS10. Raman spectra (Ram) was performed by Thermofisher DXR2. Atomic force microscopy (AFM) was employed on Si chips by a Brucker Icon AFM. Electron Paramagnetic Resonance (EPR) was performed by Brook A300.

Electrocatalytic measurements.

An electrochemistry workstation (CHI 760E) was used to evaluate OER/UOR measurements of as-prepared materials in alkaline electrolyte (1 M KOH or 1 M KOH + 0.33 M urea) with a three-electrode system. The saturated Hg/HgO electrode was used as the reference electrode. A Pt foil (1 cm*1 cm) was used as the counter electrode.

The sample modified NF was applied as the working electrode. The working electrode was prepared as follows: the NF was ultrasonicated in ethanol, 1M HCl, and Ultrapure water respectively for 20 minutes to get rid of surface impurities and remove the surface nickel oxide layer. 5 mg catalyst was dispersed in 1 mL ethanol, and then 40 μL of 5 wt.% Nafion solution was added. The Pt/C and RuO_2 electrode in the two-electrode system was prepared following the aforementioned procedure (the mass loading is 1 mg cm^{-2}). The as-prepared solution was immersed in an ultrasonic bath for at least 1h. After that, solution was sprayed onto the NF (catalyst loading 1 mg cm^{-2}). All NF electrodes loaded with catalysts were soaked in 0.1 M KOH for 30 min before measurements. All the electrochemical tests were conducted at room temperature.

UOR measurements.

An electrochemistry workstation (CHI 760E) was used to evaluate UOR measurements of as-prepared materials in alkaline electrolyte (1 M KOH + 0.33 M urea) with a three-electrode system. Convert all potentials to reversible hydrogen electrodes (RHE) according to the Nernst equation: $E_{RHE} = E_{Hg/HgO} + 0.098 + 0.059V \times PH$. Before Linear sweep voltammetry (LSV) tests, the working electrode was first activated 100 times using cyclic voltammetry (CV) tests. LSV was tested at 5 mV s^{-1} with 85% IR compensation. The Tafel slopes were obtained from the corresponding UOR-CV curves. Double-layer capacitance (Cdl) was gained through UOR-CV measurement, which was scanned at different scan rates from 10 mV s^{-1} ~ 50 mV s^{-1}. Electrochemical impedance spectroscopy (EIS) was performed at 1.40 V (vs. RHE) with an AC amplitude of 5 mV in the frequency range of 10 kHz to 0.1 Hz. Long-term stability was tested for 100 h at 10 mA cm^{-2}. Turnover frequency (TOF) values were calculated using the following equation:

$$TOF = \frac{JA}{4Fn}$$

Where J stands for the current density in ampere, A is the electrode area, F represents the Faraday's constant (96485.3 C mol^{-1}), and n accounts for the total number of moles of metal that participate in the electrocatalytic reaction. For this work, it was assumed that all the Ni metal atoms present in the catalyst participated during UOR.

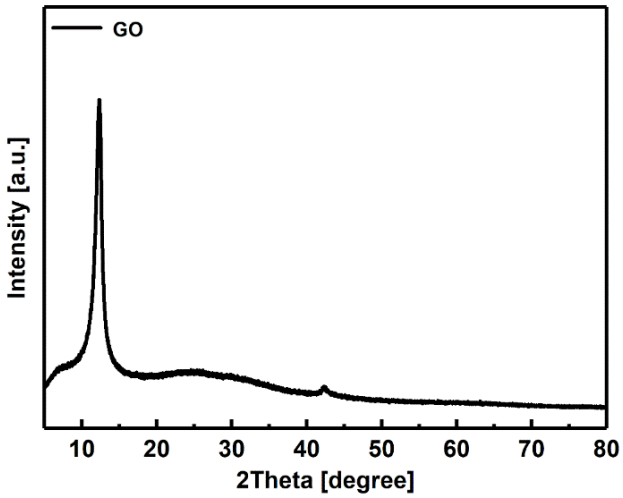

Fig.S1. XRD pattern of GO.

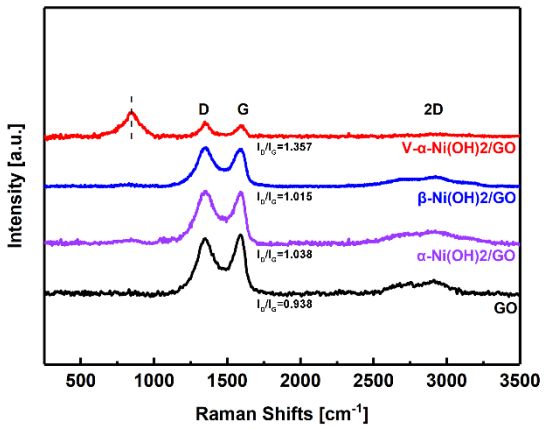

Fig.S2. Raman spectras of V-α-$Ni(OH)_2$/GO, β-$Ni(OH)_2$/GO, α-$Ni(OH)_2$/GO and GO.

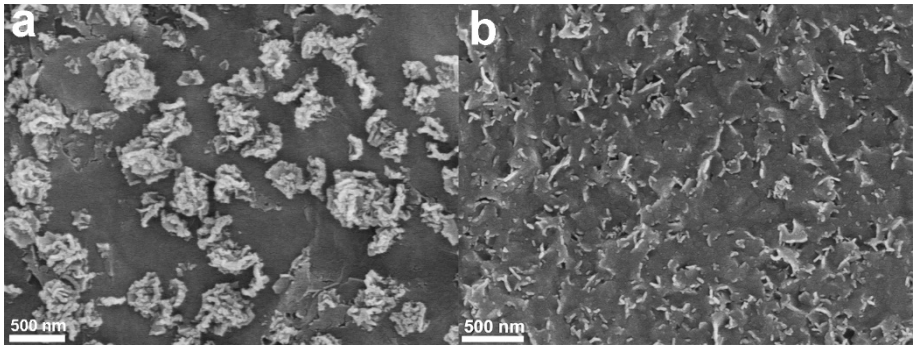

Fig.S3. SEM images of (a) α-$Ni(OH)_2$/GO, (b) β-$Ni(OH)_2$/GO

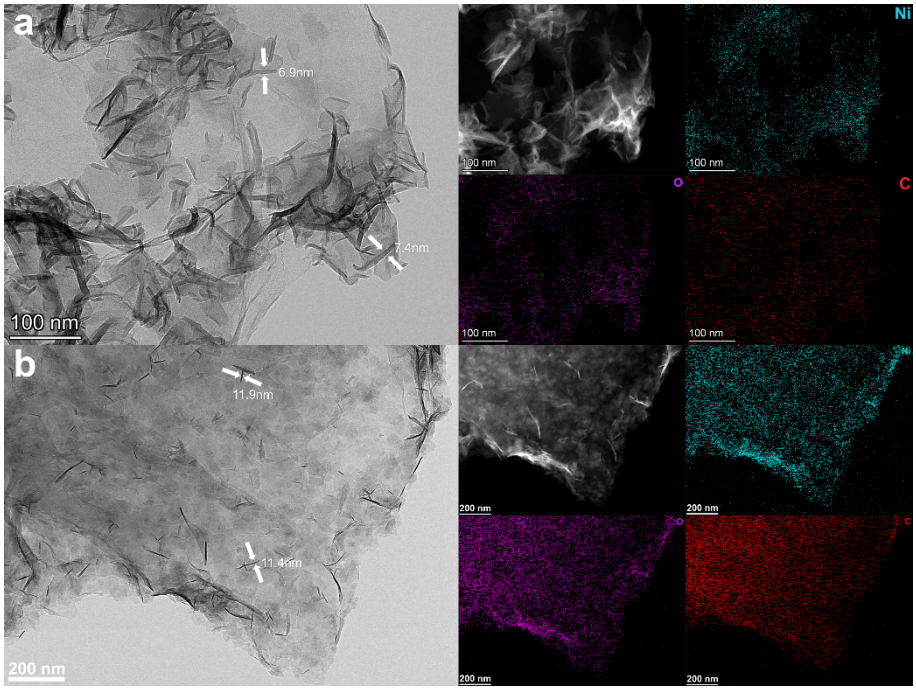

Fig.S4. TEM and element mapping images of (a) α-$Ni(OH)_2$/GO, (b) β-$Ni(OH)_2$/GO.

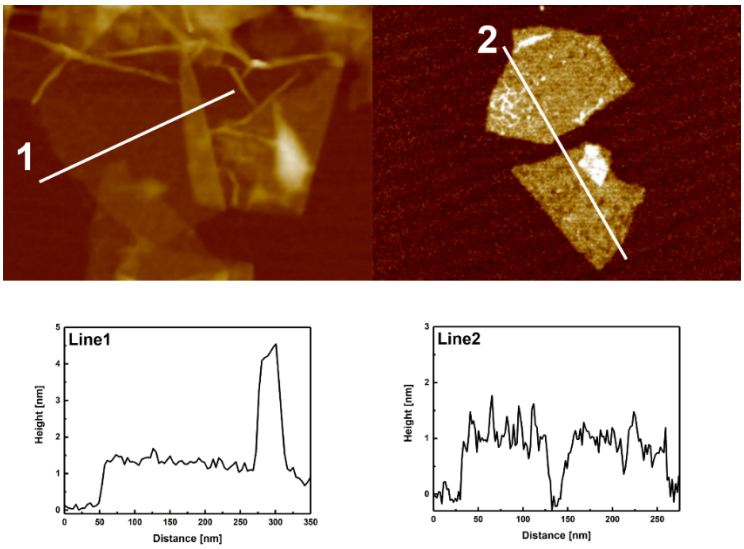

Fig.S5. AFM images of GO.

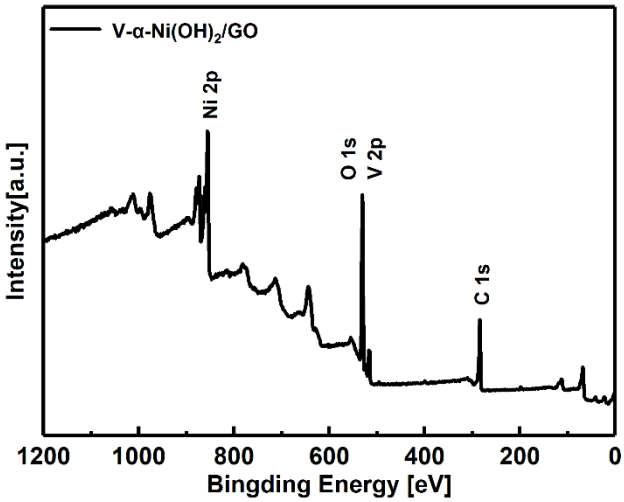

Fig.S6. XPS survey spectra of the V-α-$Ni(OH)_2$/GO.

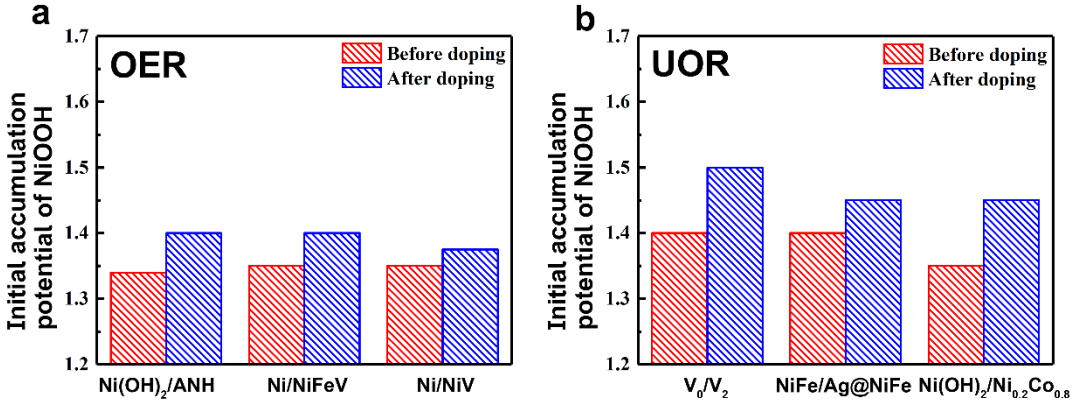

Fig.S7. The initial accumulation potential of NiOOH in (a) $Ni(OH)_2$/ANH[1], Ni/NiFeV[2], Ni/NiV[2] catalysts during OER processes, and (b) V_0/V_2[3], NiFe/Ag@NiFe[4], $Ni(OH)_2/Ni_{0.2}Co_{0.8}$[5] catalysts during UOR processes revealed by in-situ Raman spectra.

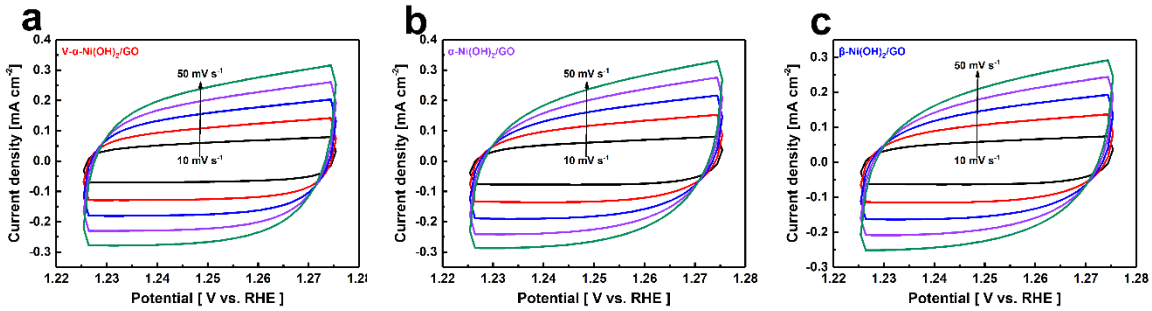

Fig.S8. CV curves of with the scan rate from 10 mV s^{-1} to 50 mV s^{-1} of (a) V-α-$Ni(OH)_2$/GO, (b) α-$Ni(OH)_2$/GO, (c) β-$Ni(OH)_2$/GO.

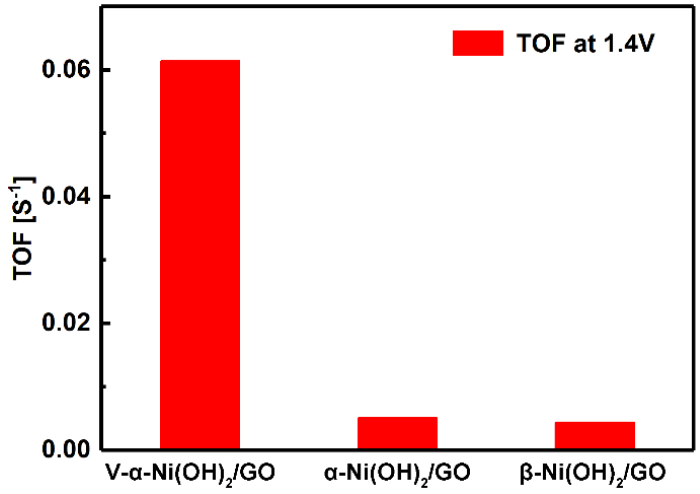

Fig.S9. Bar chart comparing the TOF of catalysts under investigation at 1.4V.

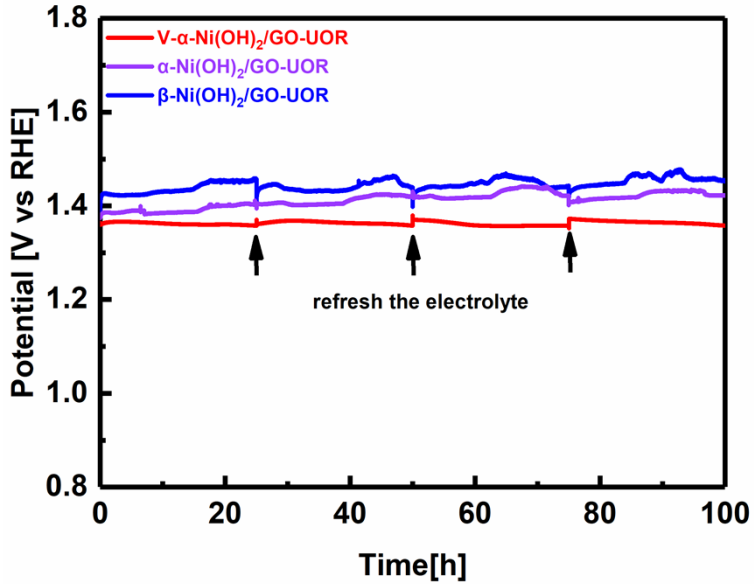

Fig.S10. Durability of V-α-$Ni(OH)_2$/GO and α-$Ni(OH)_2$/GO, β-$Ni(OH)_2$/GO.

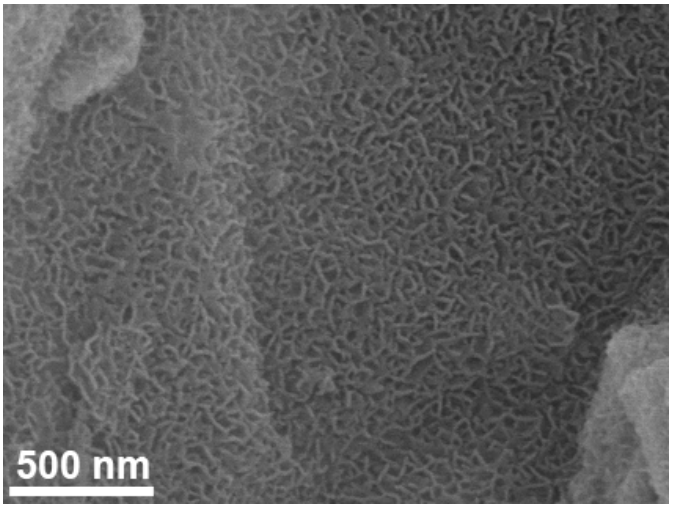

Fig.S11. SEM images of V-α-Ni(OH)$_2$/GO after UOR stability test.

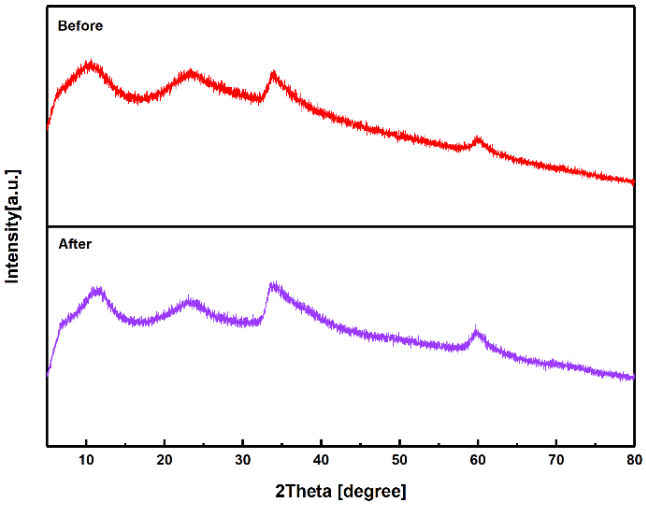

Fig.S12. XRD pattern of the V-α-Ni(OH)$_2$/GO before and after UOR stability test.

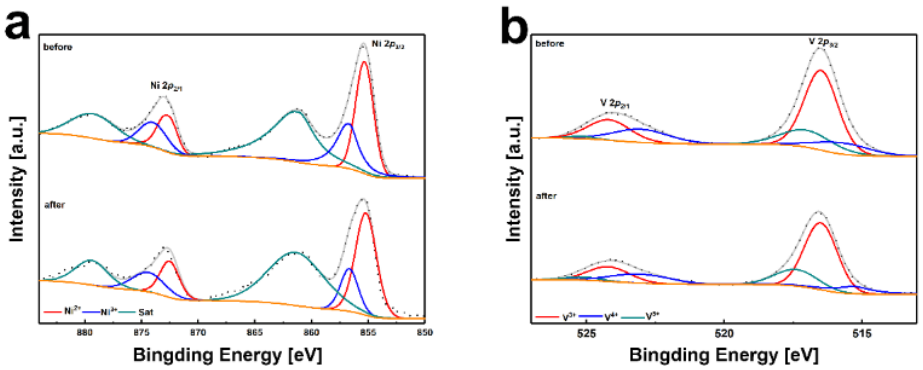

Fig.S13. (a) Ni 2p, and (b) V 2p XPS spectras of the V-α-Ni(OH)$_2$/GO after UOR stability test.

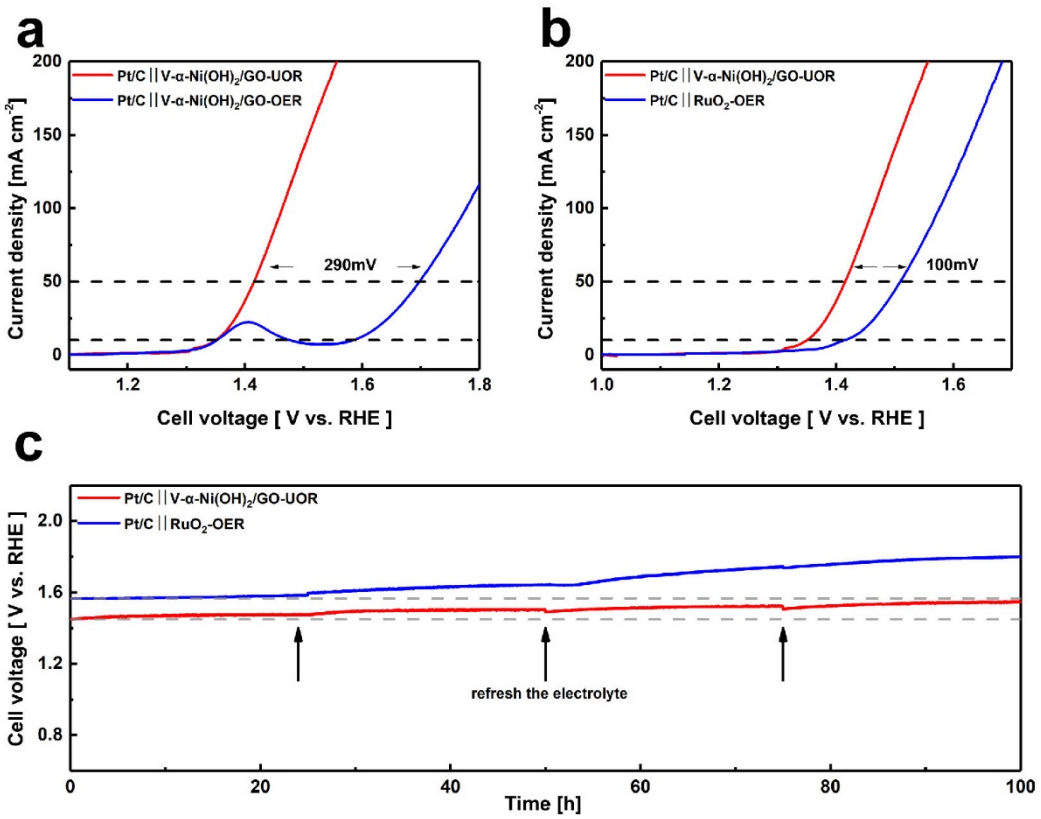

Fig.S14. (a) Polarization curves of the Pt/C//V-α-$Ni(OH)_2$/GO for urea-assisted electrolysis and water electrolysis. (b) Comparison of polarization curves, and (c) Durability recorded at 50 mA cm^{-2} in 100 h for urea-assisted electrolysis of the Pt/C//V-α-$Ni(OH)_2$/GO configuration and for water electrolysis of the Pt/C//RuO_2 configuration.

Table S1. Comparison of the effect for different metal doping $Ni(OH)_2$ on its catalytic activity.

Element	Electro-negativity	Atomic radius (pm)	Sample	Nanosheet thickness/ length (nm)	Shift in Ni^{2+}/Ni^{3+} redox peak（CV）	Improvement of UOR activity after doping [100mAcm^{-2}]
Fe[6]	1.83	156	1%Fe α-$Ni(OH)_2$/NF	＜10/150	/	225 mV
Co[7]	1.88	152	5%Co-$Ni(OH)_2$	8/200	-0.03 V	110 mV
Cu[8]	1.90	145	1%Cu α-$Ni(OH)_2$/NF	＜20/180	-0.02 V	50 mV
Mn[9]	1.55	161	Mn-$Ni(OH)_2$ PNAs	＜10/80	＜-0.05 V	65 mV

Cr[10]	1.66	166	Cr- $Ni(OH)_2$	＜10/60	-0.065 V	120 mV
V	1.63	171	α-$Ni(OH)_2$/GO β-$Ni(OH)_2$/GO V-α-$Ni(OH)_2$/GO	7.4/35 11.9/40 4-7/20	-0.01 V	310 mV

Table S2. ICP results of the V-α-$Ni(OH)_2$/GO.

Samples	Element	Concentration average[mg/L]	Ni:V ratios
V-α-$Ni(OH)_2$/GO	Ni	162.44	3:1
	V	54.586	

Table S3. Comparison of UOR performance of V-α-$Ni(OH)_2$/GO with reported electrocatalysts.

Sample	Electrolyte	Current density [100 mA cm^{-2}]	Overall voltage [10 mA cm^{-2}]	Durability	Ref.
V-α-$Ni(OH)_2$/GO	1M+0.33M	1.38 V	1.350 V	50 mA cm^{-2} for 100 h	This work
V0.12-doped $Ni(OH)_2$	1M+0.33M	1.47 V	1.50 V	1.37 V for 110 h	[11]
V_2O_3/Ni/NF	1M+0.5M	≈1.40 V	1.45 V	50 mA cm^{-2} for 20 h	[12]
NieMo nanotube	1M+0.1M	≈1.42 V	1.43 V	10 mA cm^{-2} for 24 h	[13]
NF/ P-$NiMoO_{4-x}$	1M+0.33M	1.38 V	1.48 V	10 mA cm^{-2} for 25 h	[14]
H-NiFe-LDH/NF	1M+0.33M	1.41 V	1.418 V	1.50 V for 25 h	[15]
FQD/CoNi-LDH/NF	1M+0.33M	1.42 V	1.45 V	10 mA cm^{-2} for 100 h	[16]
CoNiP@C/NF	1M+0.5M	≈1.39 V	1.43 V at 20 mA cm^{-2}	1.43 V for 60 h	[17]

MoS_2/Ni_3S_2	1M+0.5M	≈1.41 V	1.44 V	8 mA cm^{-2} for 24 h	18
P-$CoNi_2S_4$ YSSs	1M+0.5M	1.37 V	1.402 V	1.402 V for 100 h	19
NiMoV LDH/NF	1M+0.33M	1.40 V	≈1.47 V	15 mA cm^{-2} for 15 h	20

References.

1. Y. Zhu, C. Liu, S. Cui, Z. Lu, J. Ye, Y. Wen, W. Shi, X. Huang, L. Xue, J. Bian, Y. Li, Y. Xu and B. Zhang, *Adv Mater*, 2023, **35**, e2301549.
2. H. Yang, L. Ge, J. Guan, B. Ouyang, H. Li and Y. Deng, *J Colloid Interface Sci*, 2024, **653**, 721-729.
3. H. Qin, Y. Ye, J. Li, W. Jia, S. Zheng, X. Cao, G. Lin and L. Jiao, *Advanced Functional Materials*, 2022, **33**.
4. X. Zhang, J. Zhang, Z. Ma, L. Wang, K. Yu, Z. Wang, J. Wang and B. Zhao, *J Colloid Interface Sci*, 2024, **665**, 313-322.
5. X. Yang, H. Zhang, B. Yu, Y. Liu, W. Xu and Z. Wu, *Energy Technology*, 2022, **10**.
6. J. Xie, W. Liu, F. Lei, X. Zhang, H. Qu, L. Gao, P. Hao, B. Tang and Y. Xie, *Chemistry*, 2018, **24**, 18408-18412.
7. Y. Wang, Y. Lu, Y. Shi, J. Wang, Y. Zheng, J. Pan, C. Li and J. Cao, *Applied Surface Science*, 2023, **640**.
8. J. Xie, L. Gao, S. Cao, W. Liu, F. Lei, P. Hao, X. Xia and B. Tang, *Journal of Materials Chemistry A*, 2019, **7**, 13577-13584.
9. F. Chen, F. Yang, C. Sheng, J. Li, H. Xu, Y. Qing, S. Chen, Y. Wu and X. Lu, *J Colloid Interface Sci*, 2022, **626**, 445-452.
10. J. Zhang, X. Song, L. Kang, J. Zhu, L. Liu, Q. Zhang, D. J. L. Brett, P. R. Shearing, L. Mai, I. P. Parkin and G. He, *Chem Catalysis*, 2022, **2**, 3254-3270.
11. H. Qin, Y. Ye, J. Li, W. Jia, S. Zheng, X. Cao, G. Lin and L. Jiao, *Advanced Functional Materials*, 2022, **33**, 2209698.
12. Q. Zhang, B. Liu, L. Li, Y. Ji, C. Wang, L. Zhang and Z. Su, *Small*, 2021, **17**, e2005769.
13. J.-Y. Zhang, T. He, M. Wang, R. Qi, Y. Yan, Z. Dong, H. Liu, H. Wang and B. Y. Xia, *Nano Energy*, 2019, **60**, 894-902.
14. Y. Qiu, X. Dai, Y. Wang, X. Ji, Z. Ma and S. Liu, *J Colloid Interface Sci*, 2023, **629**, 297-309.
15. X. Yang, H. Zhang, W. Xu, B. Yu, Y. Liu and Z. Wu, *Catalysis Science & Technology*, 2022, **12**, 4471-4485.
16. Y. Feng, X. Wang, J. Huang, P. Dong, J. Ji, J. Li, L. Cao, L. Feng, P. Jin and C. Wang, *Chemical Engineering Journal*, 2020, **390**, 124525.
17. X. Lan, G. Li, R. Jin, X. Li and J. Zheng, *Chemical Engineering Journal*, 2022, **450**, 138225.

18. Y. Ren, C. Wang, W. Duan, L. Zhou, X. Pang, D. Wang, Y. Zhen, C. Yang and Z. Gao, *J Colloid Interface Sci*, 2022, **628**, 446-455.
19. X. F. Lu, S. L. Zhang, W. L. Sim, S. Gao and X. W. D. Lou, *Angew Chem Int Ed Engl*, 2021, **60**, 22885-22891.
20. Z. Wang, W. Liu, J. Bao, Y. Song, X. She, Y. Hua, G. Lv, J. Yuan, H. Li and H. Xu, *Chemical Engineering Journal*, 2022, **430**, 133100.